Structure-based discovery and in-parallel optimization of novel competitive inhibitors of thymidylate synthase

Donatella Tondi[1]*, Ursula Slomczynska[1†], M Paola Costi[2], D Martin Watterson[1], Stefano Ghelli[3] and Brian K Shoichet[1]

Background: The substrate sites of enzymes are attractive targets for structure-based inhibitor design. Two difficulties hinder efforts to discover and elaborate new (nonsubstrate-like) inhibitors for these sites. First, novel inhibitors often bind at nonsubstrate sites. Second, a novel scaffold introduces chemistry that is frequently unfamiliar, making synthetic elaboration challenging.

Results: In an effort to discover and elaborate a novel scaffold for a substrate site, we combined structure-based screening with in-parallel synthetic elaboration. These techniques were used to find new inhibitors that bound to the folate site of *Lactobacillus casei* thymidylate synthase (LcTS), an enzyme that is a potential target for proliferative diseases, and is highly studied. The available chemicals directory was screened, using a molecular-docking computer program, for molecules that complemented the three-dimensional structure of this site. Five high-ranking compounds were selected for testing. Activity and docking studies led to a derivative of one of these, dansyltyrosine (K_i 65 μM). Using solid-phase in-parallel techniques 33 derivatives of this lead were synthesized and tested. These analogs are dissimilar to the substrate but bind competitively with it. The most active analog had a K_i of 1.3 μM. The tighter binding inhibitors were also the most specific for LcTS versus related enzymes.

Conclusions: TS can recognize inhibitors that are dissimilar to, but that bind competitively with, the folate substrate. Combining structure-based discovery with in-parallel synthetic techniques allowed the rapid elaboration of this series of compounds. More automated versions of this approach can be envisaged.

Addresses: [1]Department of Molecular Pharmacology and Biological Chemistry, Northwestern University, Chicago, IL 60611-3008, USA. [2]Dipartimento di Scienze Farmaceutiche, Università degli Studi di Modena, 183 Via Campi, Modena, Italy. [3]Dipartimento di Chimica, Università degli Studi di Modena, 183 Via Campi, Modena, Italy.

Present addresses: *Dipartimento di Scienze Farmaceutiche, Università degli Studi di Modena, 183 Via Campi, Modena, Italy. [†]MetaPhore Pharmaceuticals Inc., 3655 Vista Avenue, St. Louis, MO 63110, USA.

Correspondence: Brian K Shoichet
E-mail: b-shoichet@nwu.edu

Key words: computer-based inhibitor design, enzyme specificity, in-parallel synthesis, structure-based drug design

Received: **21 December 1998**
Revisions requested: **27 December 1998**
Revisions received: **17 February 1999**
Accepted: **22 February 1999**

Published: **22 April 1999**

Chemistry & Biology May 1999, **6**:319–331
http://biomednet.com/elecref/1074552100500319

Introduction

If the structure of an enzyme is available, it should be possible to discover new ligands that will bind to the enzyme and modulate its action. Enzyme active sites are well formed and highly functionalized, and would seem to be good targets for such structure-based efforts. Ideally, one would like to find a new ligand scaffold and then elaborate upon it rapidly, guided by the active-site structure. Doing so is a current challenge in structural biology and medicinal chemistry.

Progress has been made in the structure-based elaboration of known lead compounds, typically substrates or substrate analogs. This has involved cycles of synthesis and structure determination [1–3], and has also drawn upon computational tools [4]. Recently, investigators have combined computational and structural approaches with combinatorial and in-parallel syntheses for focused explorations of a known lead scaffold [5,6] resulting in inhibitors up to 1000-fold more potent than the initial lead.

Nonsubstrate-like inhibitors (novel inhibitors) have also been discovered for enzymes and receptors. This has been accomplished by high-throughput screening of combinatorial, phage-display, natural-product and other libraries [7,8]. From structural studies, novel inhibitors have been discovered by molecular-docking screens of structural databases [9–12] and by *de novo* design approaches [1,13–16]. These and other [17–21] structural studies show how some enzymes recognize new inhibitors. Often, these inhibitors bind to the enzyme in orientations that differ from that adopted by the substrate or they bind to nonsubstrate sites [18,20,22–25].

In contrast to the binding heterogeneity and chemical diversity of nonsubstrate-like inhibitors, the binding orientations and chemical structures of most substrates are highly constrained; enzymes are highly specific for their substrates [26,27]. Inhibitors that do bind in substrate sites are typically substrate analogs. This might suggest a differential specificity between substrate and nonsubstrate sites for ligand chemistry or, alternatively, our notions of

Table 1

Compounds chosen from the initial DOCK screen.

Compound	Structure	IC_{50} (μM)	Dock rank
1	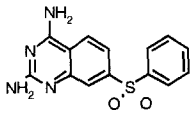	300	11
2	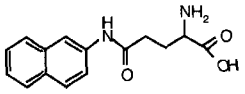	Insoluble*	78
3	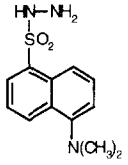	439	204
4	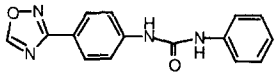	2000	226
5	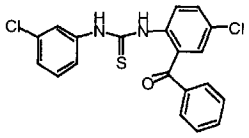	†No activity	229

*Insoluble at 50 μM. †No measurable inhibition at 50 μM.

the specificity of substrate sites might be biased by a foreknowledge of substrate structure.

We were interested in investigating the ability of a well-defined substrate site to bind molecules that are dissimilar to the substrate. To do so, we needed an approach that would suggest new scaffolds that might fit the substrate site and allow the rapid synthetic elaboration of a lead inhibitor. The following approach was adopted. To suggest new lead compounds, we screened 153,516 compounds of the available chemicals directory (ACD) of commercially available chemicals against the X-ray crystal structure of thymidylate synthase (TS) from *Lactobacillus casei* (LcTS) using the molecular-docking computer program DOCK [10]. TS catalyzes the final step on the biosynthetic pathway to thymidylate, and is consequently a target for anticancer drugs in human cells, and is a potential target for antimicrobial chemotherapy. Moreover, TS has been intensely studied as a target for structure-based inhibitor design [15], and new inhibitors have been discovered that bind to the enzyme [1,18]. Methodologically, docking screens should be unbiased by any substrate information

Figure 1

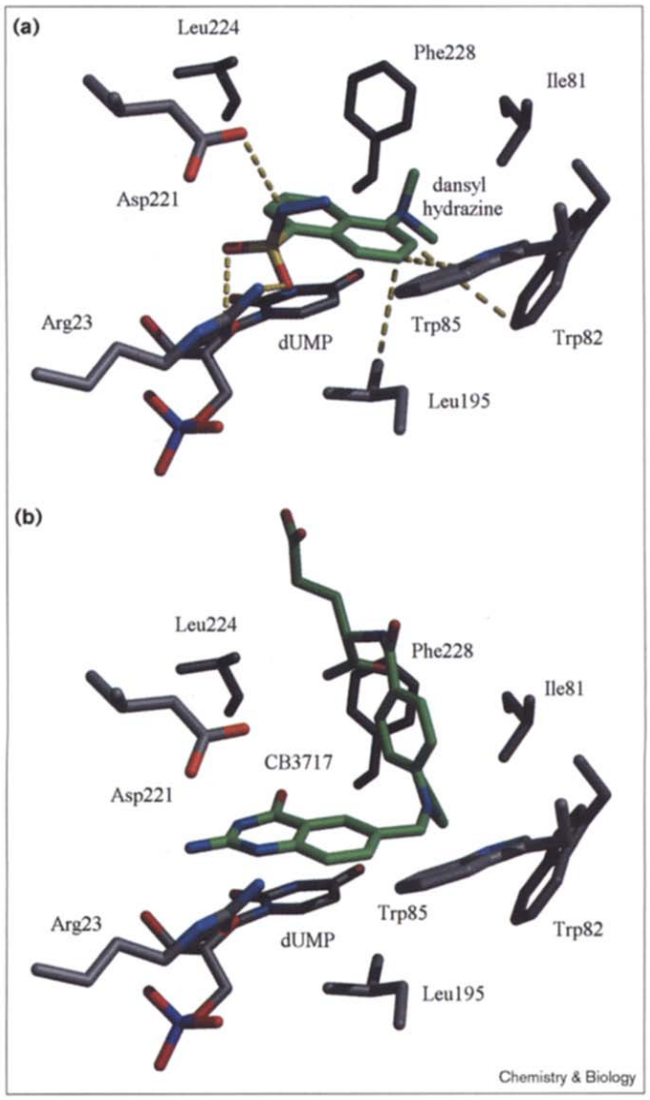

(a) The orientation of dansylhydrazine from the original docking search (carbon, green; oxygen, red; nitrogen, blue; sulfur, yellow). Residues in the binding pocket defined by CB3717 are shown and labeled, as is dUMP (carbon in gray). Several polar and nonpolar interactions are shown between LcTS and the computed orientation (dashed yellow lines). **(b)** The orientation of CB3717 in the site is shown for comparison. This figure was generated using Neon with MidasPlus [49].

other than that defined by the structure of the binding site itself; this technique has discovered new inhibitors [10] albeit ones that often bind at nonsubstrate sites [18,23,28,29]. The docking calculation was conducted against the site defined by CB3717, an analog of the substrate 5,10-methylenetetrahydrofolate (CH_2-H_4folate), in its ternary complex structure with deoxyuridine monophosphate (dUMP) and TS [30]. In this ternary complex, the enzyme has undergone a conformational change that closes down the active site on the ligands. We looked for inhibitors that acted competitively with the substrate in

Table 2

Dansyl derivatives synthesized in liquid phase.

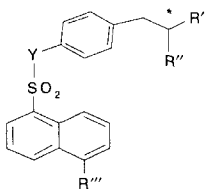

Compound	Isomer	Y	R′	R″	R‴	IC_{50} (μm)
1A	*S*	O	COOH	NH_2	$N(CH_3)_2$	163
2A	*R*	O	COOH	NH_2	$N(CH_3)_2$	220
3A	*S*	NH	COOH	NH_2	$N(CH_3)_2$	348
4A	*S*	O	COOH	NH_2	Cl	250*
5A	*S*	NH	COOH	NH_2	Cl	457
6A	*S*	O	COOH	NH_2	H	435
7A	*S*	O	COOH	$NHCOCH_3$	$N(CH_3)_2$	103
8A	*R*	O	COOH	$NHCOCH_3$	$N(CH_3)_2$	110*
9A	*S*	O	$CONH_2$	NH_2	$N(CH_3)_2$	83
10A	*R*	O	$CONH_2$	NH_2	$N(CH_3)_2$	70
11A	*S*	NH	$CONH_2$	NH_2	$N(CH_3)_2$	140*
12A	*S*	O	$CONH_2$	$NHCOCH_3$	$N(CH_3)_2$	253*
13A	*R*	O	$CONH_2$	$NHCOCH_3$	$N(CH_3)_2$	459*
14A	*S*	O	COOH	NHBOC	$N(CH_3)_2$	78
15A	*S*	O	COOH	NHFMOC	$N(CH_3)_2$	108
16A	*S*	O	$CONHCH_2CONH_2$	NH_2	$N(CH_3)_2$	196*
17A	*S*	O	$CONHCH_2COOH$	NH_2	$N(CH_3)_2$	104
18A	*R*	O	COOH	$NHSO_2$–dansyl	$N(CH_3)_2$	70
19A	*S*	O	COOH	H	$N(CH_3)_2$	74
20A†	*S*	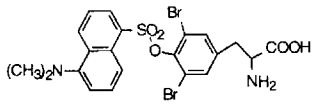				409
21A†	*S*	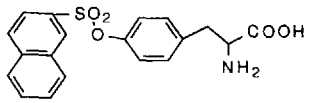				1900
22A†	*S*	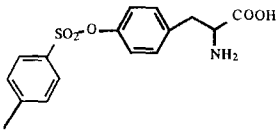				4200

*IC_{50} is approximate due to the low solubility of compound. †The entire structure is represented in the column, not just the R′ group.

enzyme assays. To allow the rapid elaboration of any inhibitor discovered, we wanted a lead compound that was compatible with solid-phase in-parallel derivatization.

We report here the discovery of a new class of antifolates that binds to LcTS at micromolar concentrations. These inhibitors do not resemble the substrate or classical antifolates; nevertheless, they are competitive inhibitors of LcTS. In this new class of inhibitors, as affinity increases so too does specificity for LcTS versus related enzymes.

Results

A list of 400 top-scoring molecules was generated by DOCK on the basis of van der Waals interactions and electrostatic interaction energy [31], both of which were corrected for ligand desolvation energy [32]. Five compounds were chosen for initial enzymatic tests from this list (Table 1). In addition to having a good DOCK score, these choices were made on the basis of the number of polar interactions observed in the docked complex and the possibility of making derivatives of a given molecule through solid-phase synthesis.

Of the molecules chosen, compound **1** (IC_{50}=300 μM) was a quinazoline that resembled CB3717 and the substrate (several more flexible quinazolines in the ACD were missed in our calculation, partly because ligand flexibility was not allowed). The similarity of compound **1** to known

Figure 2

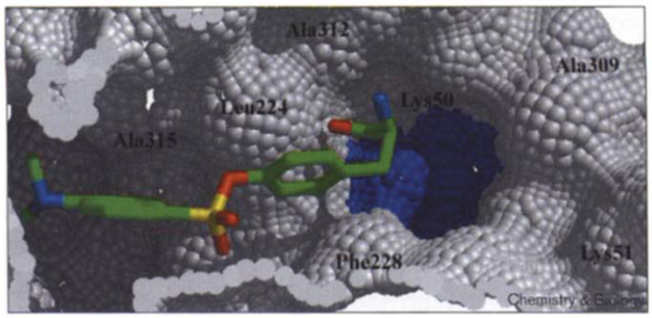

A docked orientation of dansyltyrosine in LcTS. The molecular surface of the binding site is shown in gray, except for Lys50, which is shown in blue. Key residues are labeled. The color scheme is the same as in Figure 1.

antifolates made it unappealing as a lead compound for this study. Compound **2** was insoluble in buffer. Compound **4** had very low affinity for LcTS and compound **5** was inactive at its solubility limit of 50 μM. The most interesting compound was **3**, dansylhydrazine, which inhibited TS competitively with an IC_{50} of 439 μM, did not resemble known antifolates and seemed suitable for chemical elaboration.

In the docked orientation, dansylhydrazine appears to interact with LcTS through three hydrogen bonds: ligand atom O14 (SO2)–NH1 of Arg23 (distance 3.2 Å); ligand atom O15 (SO2)–NH2 of Arg23 (distance 2.8 Å); and ligand atom NH (NH–NH2)–O of Val316 (distance 3.3 Å, Figure 1). Nonpolar contacts are also made. This geometry suggested that larger derivatives could be accommodated by the enzyme. Seven dansyl amino acid analogs, representing a range of sulfonyl derivatives, were tested against LcTS (see the Supplementary material). Among these, *O*-dansyl-L-tyrosine (**1A** in Table 2, dansyltyrosine) was a competitive inhibitor of LcTS with an IC_{50} value of 163 μM and a K_i value of 65 μM.

We explored the structural bases for the activity of dansyltyrosine. Low-energy conformations of the molecule (500) were calculated [33] and docked into the folate-binding

Figure 3

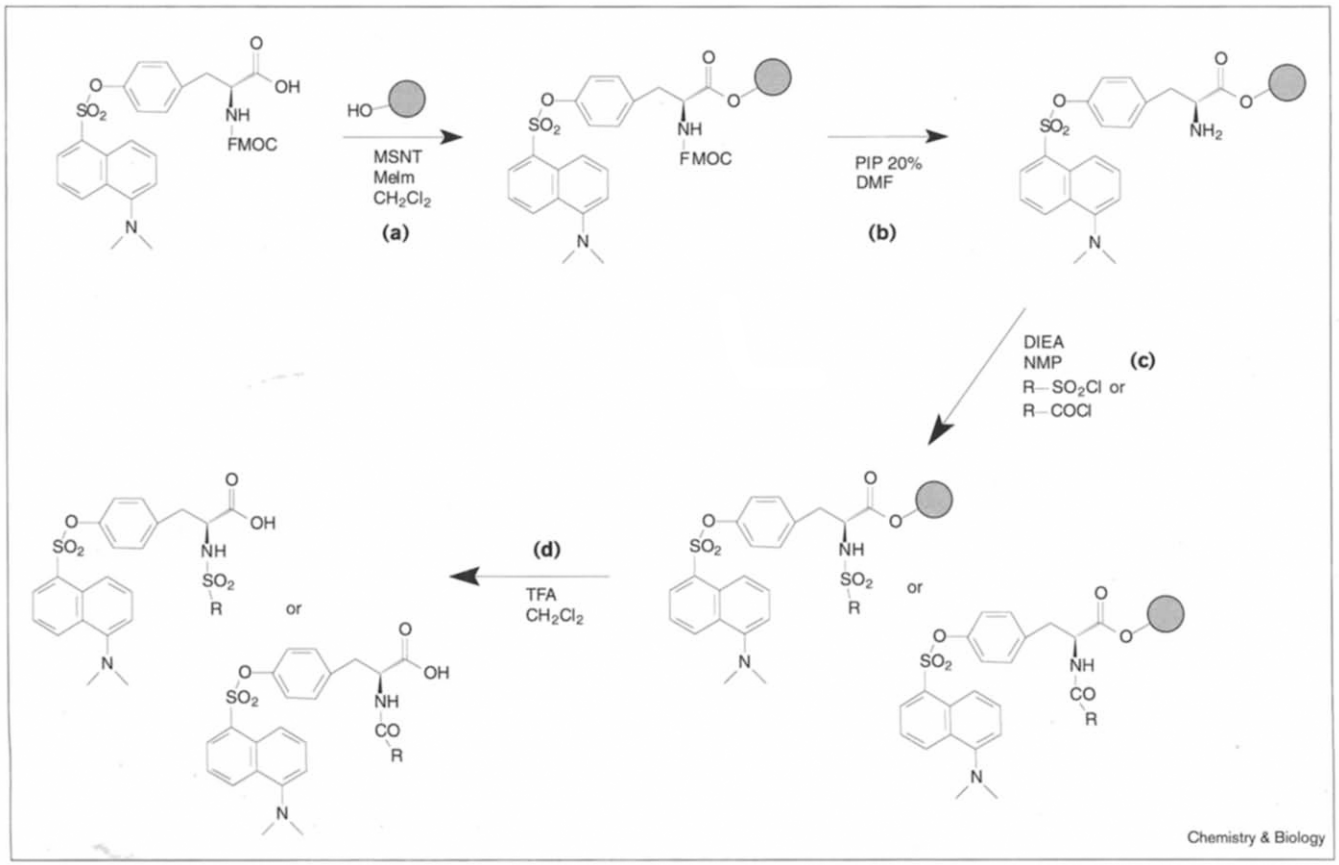

In-parallel solid phase synthesis of dansyltyrosine derivatives. Reagents and conditions: **(a)** MSNT, MeIm, CH_2Cl_2, room temperature. **(b)** 20% PIP, DMF, room temperature. **(c)** DIEA, NMP, room temperature. **(d)** TFA, CH_2Cl_2, 2 h, room temperature.

Table 3

Derivatives of dansyltyrosine synthesized in parallel.

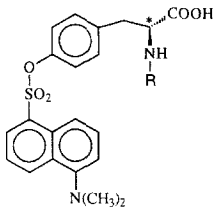

Compound	R Group	IC_{50} (μM)	Compound	R Group	IC_{50} (μM)
1B	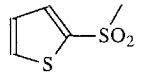	86	**14B**		21
2B	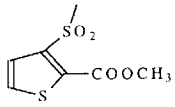	25	**15B**	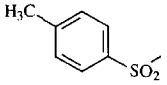	20
3B	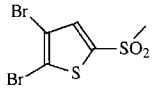	109	**16B**	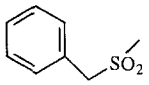	19
4B	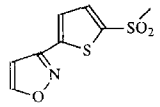	8.8	**18B**†	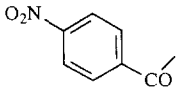	60
5B	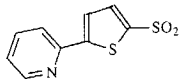	16.7	**19B**	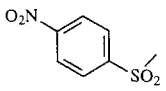	10
6B	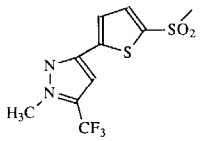	68*	**20B**	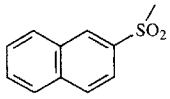	4.7
7B	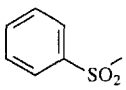	67	**21B**	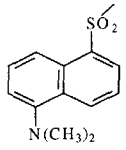	3.4
8B	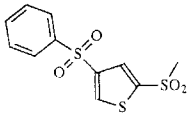	101	**22B**	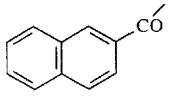	70
9B	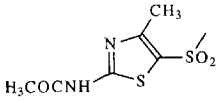	256	**23B**	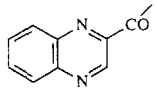	34
10B	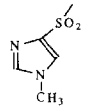	49	**24B**	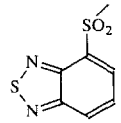	10
11B	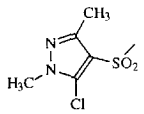	161	**25B**	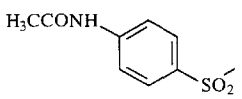	29
12B	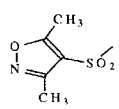	138	**26B**	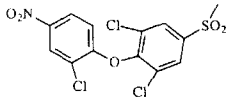	>>50‡
13B	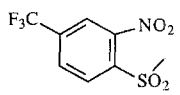	27	**27B**	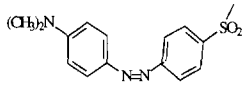	>>100§

Table 3 cont'd

Derivatives of dansyltyrosine synthesized in parallel.

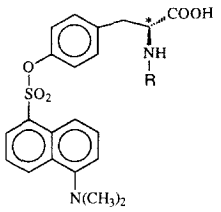

Compound	R Group	IC_{50} (μM)	Compound	R Group	IC_{50} (μM)
28B	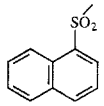	10	**32B**	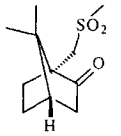	86
29B	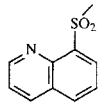	7	**33B**	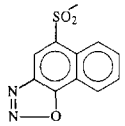	13.5
30B	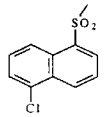	11	**34B**	$F_3C\text{-}CH_2\text{-}SO_2$	90
31B	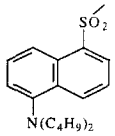	53*			

*Estimated due to low solubility of this compound. †**17B** was not tested because of the low reaction yield. ‡No activity detected at 50 μM. §No activity detected at 100 μM.

site. The resulting configurations clustered into two orientations. In one orientation, the tyrosine group overlaps the quinazoline ring of CB3717. In the second cluster of orientations, the dansyl sulfone group overlaps the quinazoline ring of CB3717, making hydrophobic contacts with the surrounding residues (Trp85, Trp82, dUMP, Ile81, Phe228 and Leu224). An apparent hydrogen bond is made between the carboxylate group of the tyrosine amino acid moiety and the Nζ of Lys50 (O6–Nζ distance 2.7 Å; O7–Nζ distance 2.8 Å; Figure 2).

Although we cannot distinguish between these two possibilities unambiguously, structure–activity relationships favor the dansyl group acting as the anchor fragment, binding in the quinazoline site, as suggested by the second cluster of orientations. For example, tyrosine derivatives had no inhibitory activity against TS, whereas dansyl derivatives were active. Molecules that changed the geometry around the naphthyl ring lost almost all activity (compounds **21A** and **22A**; Table 2). Converting the zwitterionic amino acid into a compound that bore a formal charge, either by acylating the amino group (compounds **7A** and **8A**) or by amidating the carboxylate (compounds **9A** and **11A**), led to inhibitors with up to twofold improved activity. Derivatives with both substitutions were less active by twofold to threefold (**12A** and **13A**). The amino group seemed to accommodate larger substituents (**14A** and **15A**) than did the carboxylic acid (**16A**). None of these observations was compelling by themselves, but taken together they suggested amino derivatives of *O*-dansyl-L-tyrosine could be favorably accommodated by LcTS.

A small library of 33 amino derivatives of *O*-dansyl-L-tyrosine was synthesized using solid-phase in-parallel chemistry (Figure 3). These compounds inhibited LcTS with IC_{50} values ranging from 3.4 to 256 μM (Table 3). The most potent of these compounds, *N*,*O*-didansyl-L-tyrosine (**21B**, didansyltyrosine), had a K_i of 1.3 μM. This compound was a competitive inhibitor of TS versus CH_2-H_4folate (Figure 4) and was noncompetitive versus the second TS substrate, dUMP, which binds at a second site (data not shown). Ten other compounds had IC_{50} values of less than 20 μM, which, assuming competitive inhibition, suggests that they have K_i values of less than 10 μM. One of these, **20B**, was explicitly shown to be competitive with a K_i of 1.7 μM (data not shown).

To construct a model for how didansyltyrosine (**21B**) bound to LcTS further docking calculations were performed. Low

Figure 4

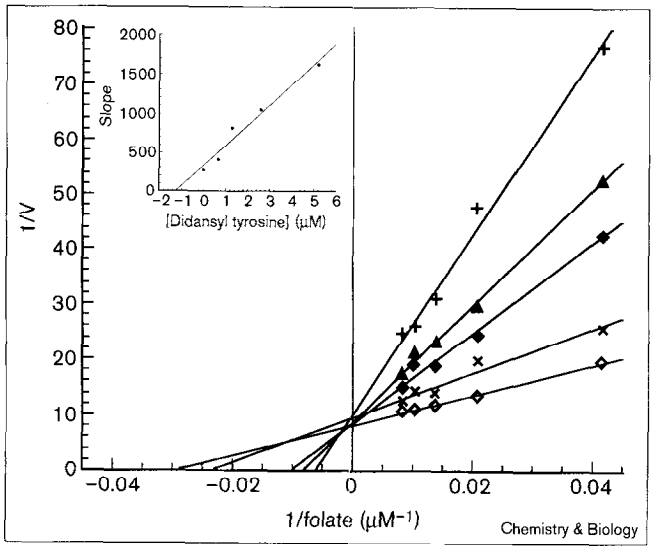

Lineweaver–Burk plot for didansyltyrosine (**21B**). The concentrations of inhibitor used were 0 μM (open diamonds); 0.67 μM (X); 1.3 μM (filled diamonds); 2.6 μM (filled triangles); 5.2 μM (+). The Y axis is $(OD_{340}/min)^{-1}$. The inset shows the re-plot of the slopes, giving a K_i of 1.3 μM.

energy conformations of the molecule (500) were generated [33] and docked into the binding site. Several families of orientations of didansyltyrosine were found that fit the enzyme well. Most position the original dansyl group in the quinazoline site of LcTS (Figure 5a,b). In the orientation shown in Figure 5a, this anchor dansyl ring makes nonpolar interactions with the pyrimidine ring of dUMP (distances are C45–O4 of dUMP 3.4 Å; C42–N1 of dUMP 4.51 Å; C42–C6 of dUMP 4.21 Å). The dansyl ring also makes nonpolar contacts with folate-binding residues, including C35-Cγ2 of Ile81 4.0 Å, C45–NH2 of Arg23 4.0 Å, C42–Cβ of Ala315 3.9 Å, and C45–Cδ1 of Leu195 4.5 Å.

As the inhibitor extends out of the quinazoline-binding site of LcTS, the active-site cleft opens up (Figure 6), leaving room for more orientations of the flexible *N*-dansyltyrosine group. In most orientations, the tyrosine ring interacts with hydrophobic residues such as Phe228 and Leu224. In the orientation represented in Figure 5a, for instance, four tyrosine-ring atoms interact with Phe228 at distances ranging from 3.3 to 3.8 Å, and three ring atoms interact with Leu224 at distances ranging from 3.2 Å to 3.6 Å. In this orientation, the tyrosine carboxylate maintains its interaction with Lys50 (O22–Nζ of Lys50 2.8 Å). In other high-scoring orientations this interaction is lost, and the carboxylate extends out towards the solvent.

The conformation of the second dansyl group varies most in the docked orientations, falling as it does in the most open part of the site (Figure 6). Among the most energetically favorable configurations is that which places this ring

Figure 5

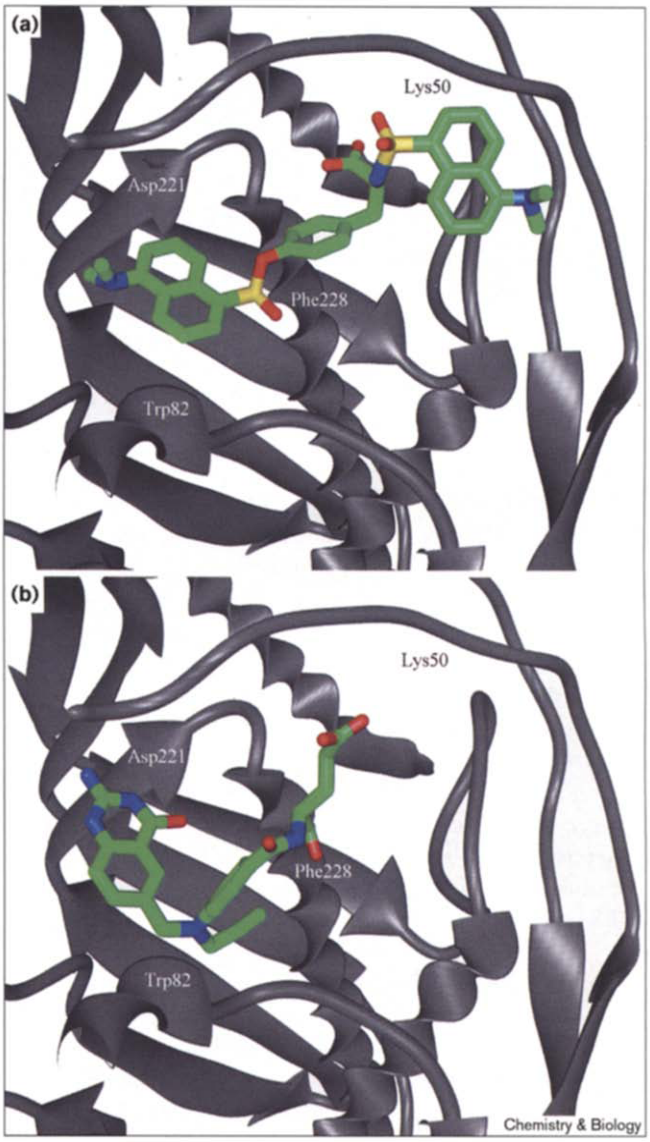

Didansyltyrosine docked into the folate-binding site of LcTS (colored as in Figure 1). **(a)** The docked orientation of didansyltyrosine in LcTS. **(b)** The crystallographic structure of CB3717 in LcTS.

so as to interact with residues Ala309 (ligand C12–Cβ 3.5 Å and ligand C6–Cβ 3.7 Å) and Ile310 (ligand C8–O 3.4 Å) and with Lys51 (ligand C17–Nζ 4.1 Å), at the mouth of the active site (Figure 5a). In a second family of favorable conformations, the second dansyl ring packs against a hydrophobic patch at the mouth of the active site, interacting with Leu56 (3.1 Å), Ile81 (3.5 Å) and the Cβ of His80 (3.2 Å). In this orientation, the dimethyl amino group of the second dansyl ring points towards residues of the small domain of LcTS, and is within 4.5 Å of this region.

Although the molecules from the in-parallel optimization had higher affinities for LcTS than did the lead compounds,

Figure 6

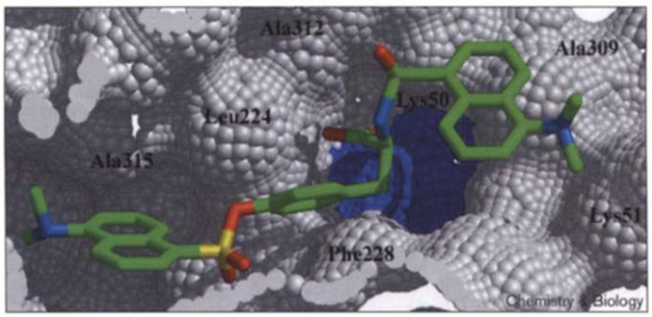

A docked orientation of didansyltyrosine (**21B**) in LcTS showing the fit to the overall binding site (colored as in Figure 1). The molecular surface of the enzyme is shown in gray, except for Lys50, which is colored in blue. Several key residues are labeled.

Figure 7

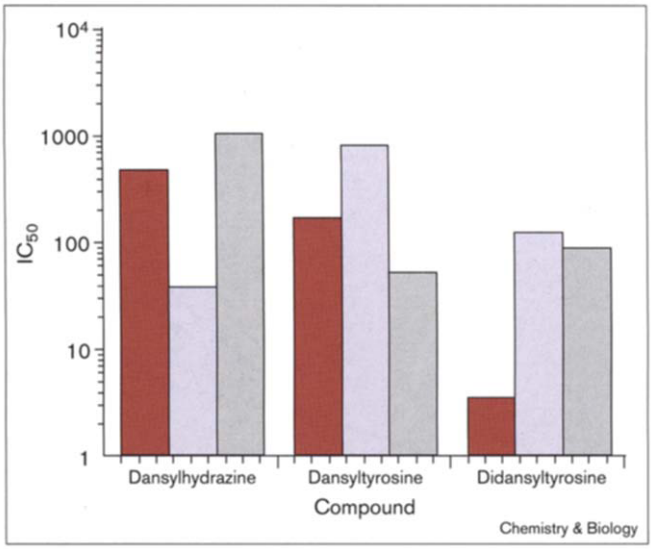

The specificity of the dansyltyrosine analogs for LcTS versus HTS and chymotrypsin. Activity against LcTS (red), HTS (blue) and chymotrypsin (gray).

they were also larger and more hydrophobic. To examine whether the affinity of these compounds correlated with their hydrophobicity, the logP of the compounds was calculated [34]. We observed no correlation between affinity and hydrophobicity using this measure (data not shown). To investigate how specificity for LcTS changed with affinity in the dansyltyrosine family, the activity of these compounds was measured against human TS (HTS), the folate-converting enzyme dihydrofolate reductase (DHFR), and chymotrypsin, which recognizes hydrophobic ligands [35] (Figure 7). The lead compound, dansylhydrazine, is 13-fold less selective for LcTS than for HTS. Dansyltyrosine, on the other hand, is fivefold more selective for LcTS than for HTS but still has an IC_{50} of 50 μM for chymotrypsin, which is threefold better than for LcTS. Finally, didansyltyrosine is 30-fold more selective for LcTS than for HTS and 25-fold more selective for LcTS than for chymotrypsin. The K_m values of folate for HTS and LcTS are both around 10 μM, so that the IC_{50} ratios (Figure 7) probably reflect K_i ratios, although we have not measured K_i values for HTS directly. None of the three compounds shows any affinity for DHFR at the maximum concentrations allowed by solubility. In the dansyltyrosine family of LcTS inhibitors, specificity and affinity appear to rise together.

Discussion

Our interest was to probe a substrate-binding site for its ability to bind new inhibitors in a manner that allowed rapid elaboration of a lead compound. It is appropriate to ask whether didansyltyrosine and its congeners are genuinely binding at the folate site of LcTS, and whether they are doing so in a specific manner. If the didansyltyrosines are binding specifically to the folate site, how different are they from the substrate and known antifolates, that is, are they genuinely novel?

Didansyltyrosine (**21B**) inhibits LcTS competitively with CH_2-H_4folate (Figure 4) and noncompetitively with the nucleotide substrate dUMP, as does its analog **20B** and as does dansyltyrosine itself. We suspect that most of the in-parallel library members would show the same behavior. These kinetic data do not prove that the inhibitors are binding at the folate site; formally, competitive inhibition only implies binding to the same state of the enzyme to which the folate binds. Still, it seems likely that didansyltyrosine binds to the closed conformation of LcTS at the folate site, given this inhibition pattern. Even inhibitors that bind only partially to the folate site, such as phenolphthalein, show a mixed inhibition pattern versus CH_2-H_4folate [18].

One indication of specific binding is that small changes among the dansyltyrosine derivatives can have a large effect on activity (Table 3). For instance, converting a sulfonamide into an amide (compound **16B** versus **18B**, or **20B** versus **22B**) diminishes activity by sixfold to 15-fold. In a larger change, adding an isoxazole ring to **1B** (to make compound **4B**) improved affinity tenfold. Although larger derivatives are often more active than the smaller ones, neither size nor hydrophobicity is enough to explain binding; there is no correlation between binding affinity and ClogP value. For instance, the amide analogs have higher ClogP values but are considerably less potent than their sulfonamide congeners. Similarly, compound **29B** (ClogP 5.2) is less hydrophobic but more active than the similar inhibitors **28B** (ClogP 6.2), **30B** (ClogP 7.0), and **31B** (ClogP 9.3). Not every large change led to a significant effect, however. For example, compound **33B** has almost the same affinity for LcTS as does compound **28B**, even though a third ring has been added to the former.

Some of the functionality explored in these compounds might well be only loosely associated with the enzyme.

Although there is no overall correlation between hydrophobicity and activity, the most active inhibitor, didansyltyrosine (**21B**), is among the most hydrophobic. Often, a substrate can be turned into an inhibitor, or an inhibitor made more potent, by adding large hydrophobic groups to a core scaffold. This can reduce specificity for related receptors or enzymes [36]. Because our interest was to explore the chemical diversity allowed within a particular site, it seemed prudent to investigate how the specificity of the dansyl derivatives related to their affinity for LcTS. Moving from the initial, low-affinity lead compound dansylhydrazine to the more active dansyltyrosine and finally to didansyltyrosine, specificity for LcTS improved over 400-fold versus the highly related enzyme HTS. Specificity for LcTS improved by two orders of magnitude versus the hydrophobic recognizing enzyme chymotrypsin [35] (Figure 7). In other docking studies, we have found that hydrophobic ligands will often inhibit chymotrypsin (data not shown), making this a useful, if not decisive, control for this series of inhibitors. The elaboration of the lead compound resulted in not only more potent inhibitors, but also more specific inhibitors. This is consistent with binding at a specific site on LcTS. Didansyltyrosine (**21B**) is more specific for LcTS than are most antifolates which typically show little specificity for TS enzymes from different species [37,38].

Didansyltyrosine (**21B**) appears to bind specifically to LcTS, and it would be interesting to understand the particular interactions that it makes with the enzyme. To model these interactions, we docked multiple conformations of didansyltyrosine into LcTS, and looked for conformations with favorable fits that could also explain the structure–activity data. There is considerable overlap between the docked orientations of didansyltyrosine and the crystallographic orientation of CB3717 (Figure 5). The docked conformations usually bury the first, *O*-linked dansyl ring in the quinazoline-binding site of LcTS, consistent with the anchor role of this ring in the structure–activity experiments. In these orientations, the dansyl moiety makes nonpolar interactions with dUMP, suggesting that dUMP would be able to form a ternary complex with LcTS and didansyltyrosine. The first dansyl ring also interacts with active-site residues such as Ile81, Ala315 and Leu195. Most docked orientations appear to form interactions between the tyrosine ring of didansyltyrosine (**21B**) and Phe228 and Leu224 of LcTS (Figure 5).

The active site, which is constricted in the quinazoline-binding site, opens up in the region where the second dansyl ring docks, and the docking program finds several high scoring, dissimilar fits for this inhibitor moiety. Many orientations bury this dansyl ring against nonpolar surface area in the LcTS structure, consistent with the high affinity of this hydrophobic sidechain. Two such nonpolar patches stand out: that defined by Ala309 and Leu310 (Figure 5a), and that defined by Leu56, Ile81 and the Cβ of His80. We cannot reliably distinguish between these orientations on the basis of docked energies alone [39]. Considering the structure–activity data of the ligands, orientations that fit the second dansyl ring against the nonpolar patch defined by Leu56 and Ile81 are consistent with some of the variations that we observe. For instance, there is little room for large substitutions off the dimethyl amino group of the second dansyl ring in this orientation. This would explain the lower activity of the dibutyl derivative (**31B**), and compounds **26B** and **27B**, all of which would have steric clashes with enzyme residues in this orientation.

No single docked orientation of didansyltyrosine explains all of the binding data. For instance, it is not clear why the affinity of **4B** is 12-fold higher than **3B** (Table 3). Similarly, the docked structures do not explain why the sulfonamide inhibitors should always bind better than their amide analogs (Table 3). Partly, these ambiguities reflect the 'low resolution' accuracy of our docking algorithm [39], which can sometimes correctly predict the gross features of a binding complex, such as the overall placement of a ring, but miss detailed features, such as hydrogen bonding and conformational accommodation [18,40]. Partly, these ambiguities might be due to the genuine ability of different didansyltyrosine analogs to occupy different configurations in the LcTS- binding site. Such multiple binding modes have been reported previously for other inhibitor classes for this enzyme [41,42]. A very detailed description of the binding of didansyltyrosine with LcTS awaits an experimental structure determination. For now, several features could be summarized from the docking and structure–activity studies. The didansyl tyrosine analogs appear to bind in the folate-binding site of LcTS, with the first, *O*-linked dansyl ring in about the same position as the quinazoline ring of CB3717, interacting with dUMP and folate-binding residues. The tyrosine ring of the inhibitors appears to interact with residues Phe228 and Leu224. The docking studies allow the second, *N*-linked dansyl ring to be in several positions; we favor those that place it in hydrophobic patches such as that defined by Ala309 and Leu310, or that defined by Leu56 and Ile81.

As a final question, it is appropriate to ask how different are the dansyltyrosine analogs from known antifolates. In Figure 8 we present several known antifolates and the substrate CH_2-H_4folate, alongside didansyltyrosine. Without resorting to diversity metrics, it can be seen that the dansyltyrosine analogs differ from the classical antifolates, such as CB3717 and ZD1694. The dansyltyrosines lack the quinazoline ring that is highly conserved among most antifolate inhibitors of TS, and they do not possess a glutamic acid peptide tail.

Figure 8

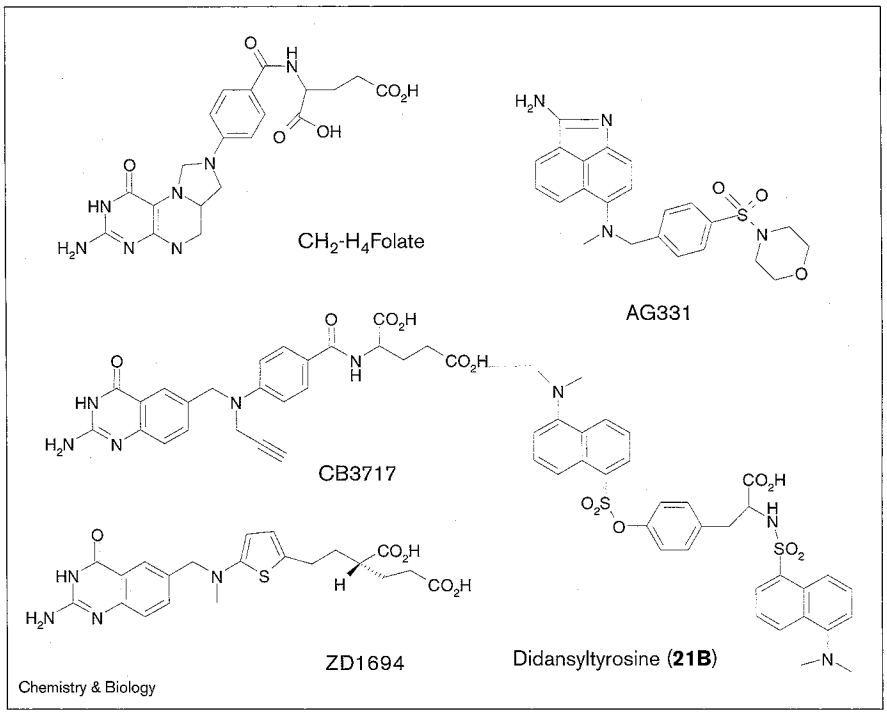

Comparing the structure of didansyl tyrosine to known inhibitors of TS.

Molecules that bear little resemblance to substrates can bind to the folate site of LcTS. This is consistent with earlier results with non-antifolate inhibitors of HTS [1,18]. Although LcTS is in many ways a highly specific enzyme [27,43], the folate site can recognize different inhibitor scaffolds. More broadly, these results are consistent with recent structural and screening work, in which diverse ligands have been found to bind at conserved ligand-recognition sites in proteins [1,24,44,45]. Substrate sites on enzymes might allow considerable diversity among inhibitor molecules.

As a technical matter, combining structure-based discovery with in-parallel synthetic elaboration exploits the complementarity between the two techniques. Previous studies have shown that structural data can constrain and guide the combinatorial elaboration of known lead compounds [5,6]. Here we drew on the ability of molecular docking to discover a new scaffold and then used in-parallel techniques to elaborate upon it rapidly. Our combination of the two techniques was crude — we merely insisted that any lead compound have a chemistry that would allow in-parallel elaboration and then used the enzyme structure as guide to model increasingly complex inhibitors. More sophisticated algorithms for combining structure-based discovery with exploration of diversity are being investigated in several laboratories; this pilot study suggests that such algorithms might be practical.

Significance

Substrate sites on enzymes are attractive targets for structure-based inhibitor design. Two difficulties hinder efforts to discover and elaborate new inhibitors that bind at these sites. First, nonsubstrate-like inhibitors often bind at nonsubstrate sites. Second, novel scaffolds frequently introduce chemistry that is unfamiliar, making synthetic elaboration challenging. In an effort to discover and elaborate a new scaffold for a substrate site, we combined molecular docking with in-parallel synthetic elaboration. We targeted the folate-binding site of thymidylate synthase, from *Lactobacillus casei*, which has been well-studied for structure-based drug design. TS catalyzes the final step on the biosynthetic pathway to thymidylate, and is consequently a target for proliferative diseases. The site was found to recognize molecules that were dissimilar to the folate substrate. Dansyltyrosine derivatives have no obvious similarity to the cognate ligand but nevertheless bind to *L. casei* thymidylate synthase (LcTS) with micromolar affinities. Small differences between related analogs can have significant effects on binding. Higher affinity is correlated with greater specificity for LcTS versus related enzymes. Nonfolate analog inhibitors have also been found to bind in the folate site of human thymidylate synthase (HTS) [1], and diverse ligands have been found to bind at conserved ligand recognition sites in other proteins [24,44,45]. Even at substrate sites, at least in some proteins, several fundamentally different chemical scaffolds can be recognized.

In-parallel and combinatorial synthetic techniques seem complementary to structure-based methods. Studies from several groups suggest that structural information can usefully constrain the diversity available in combinatorial explorations of known lead compounds [5,6]. We used a simple approach to combine the two techniques to explore the chemistry of a new scaffold. More automated methods can be envisaged.

Materials and methods

Computational work

The structure of LcTS in complex with dUMP and CB3717 (a 5,10-propargyl-quinazoline derivative of folate) was used as the basis for computational studies [30]. Potential binding sites for ligand atoms were defined by a set of 64 atoms from the folate analog CB3717 and phenolphthalein [18] from their respective complexes with LcTS. The phenolphthalein coordinates were generated in the TS ternary complex site by rigid-body fitting the Cα atoms of the phenolphthalein complex with LcTS onto the CB3717 Cα coordinates. Four of the phenolphthalein atoms were not used because of bad contacts with the protein in its ternary complex conformation. All bound water molecules were deleted.

We explored the active site of the enzyme with a modified version of DOCK3.5 [32] and a 153,516 subset of the ACD/95.2 database of commercially available compounds (MDL Inc, San Leandro CA). Partial atomic charges and van der Waals parameters for each database molecule were calculated [31]. Approximately 500 orientations were calculated for each database molecule. Each orientation of each ligand was filtered for steric fit to LcTS with a DISTMAP grid [46] with polar and nonpolar contact limits of 2.4 Å and 2.8 Å, respectively. Close contacts were disallowed. Orientations that passed this steric filter underwent up to 250 steps of simplex minimization [47] using a van der Waals and an electrostatic potential as calculated by CHEMGRID [31] and DelPhi [48], respectfully. Energies of interaction were corrected for ligand desolvation energies [32]. The calculation took four CPU days on a 250 Mhz Indigo2 R4400 SGI workstation.

Complexes for the best-scoring 400 compounds were evaluated using MIDAS-Plus [49]. On the basis of the DOCK score, the number of specific interactions with the protein, and the ease of synthetic elaboration, five compounds were tested for the ability to inhibit LcTS (Table 1). To allow more detailed structural modeling, multiple conformations of dansyltyrosine and didansyltyrosine (**21B**) were generated using SYBYL 6.3 (Tripos, St. Louis MO) and docked into LcTS. Conformations were generated by rotating all single, nonterminal bonds in increments of 120° [33]. Each conformer was independently docked as above. The hydrophobicity of the R groups in compounds **1B** to **34B** (Table 3) was calculated using the ClogP method [34].

Synthetic chemistry

N-Fmoc-tyrosine was purchased from Advanced ChemTech; *N*-Boc-tyrosine, sulfonyl chlorides and acid chlorides were purchased from Aldrich, Maybridge International, TCI-US and Lancaster. TentaGel S PHB-Wang equivalent resin (OH, 0.24 mmol/g), Tentagel Rink Amide (NH2, 0.26 mmol/g) and Rink Amide (NH2, 0.81 mmol g) resins [50] were purchased from Advanced Chemtech. The purity of all synthesized compounds was determined by using thin layer chromatography (TLC) and high performance liquid chromatography (HPLC). For TLC, 250 nm silica gel precoated uniplates (Analtech) were used with the appropriate solvent system. The chromatograms were visualized at 254 nm. HPLC was performed on a Rainin instrument using a Spheri-5 Cyano 5 micron cartridge (220 × 4.6 mm) at flow rate 0.8 ml/min; UV detection was at 300 nm, and solvents (A; 0.1% triflouroacetic acid in water) and (B; 0.08% triflouroacetic acid in acetonitrile/water; 9:1; gradient 10% to 90% B in 25 min). Structures were characterized using nuclear magnetic resonance (NMR) spectroscopy and mass spectrometry (see the Supplementary material section).

The synthesis of 22 dansyl amino derivatives (Table 2) was accomplished in liquid phase (see the Supplementary materials section). The in-parallel synthesis was carried out on an Advanced ChemTech 357 MPS using solid-phase methods (Figure 3, Table 3). *N*-Fmoc-O-dansyltyrosine was loaded on the Wang Resin-OH as described [51]. The synthesis was carried out using 4.25 g (1.02 mmol) of the TentaGel Wang Resin that was pre-washed with dry dichlormethane (DCM) three times. The dry *N*-Fmoc-dansyltyrosine (3 eq., 3.06 mmol, 1.955 g), was dissolved in DCM with 1-methyl-imidazole (2.25 eq., 2.29 mmol) in a septum-stoppered flask. The solution was then transferred to a stoppered flask containing MSNT (3 eq., 3.06 mmol, 0.816 g) in DCM, and the mixture was added to the hydroxymethyl polystyrene support Wang resin. The first coupling was carried out with continuous mixing for 3 h. Reactants were washed out first with dimethylformamide (DMF) and then with DCM. A second coupling with fresh reagents was performed for 2 h under the same conditions. The resin was divided in the 34 vessels and washed twice with DMF and DCM. The resin was then reacted with acetic anhydride and diisopropylethylamine (DIEA) (tenfold excess) in DCM for 1 h to cap the unreacted hydroxyl groups on the resin (the loading was determined based on the UV absorption of the dibenzofulvene group after Fmoc deprotection). The Fmoc group was deprotected with 30% v/v piperidine (PIP)/DMF for 3 min followed by another treatment with fresh reagent for 12 min. After washing with DMF (1 min), methanol (1 min), DMF (1 min), and NMP (1 min), the O-dansyltyrosine-carboxy-resin was reacted with 34 different sulfonyl chloride or carbonyl chloride groups. The reaction was carried out with three equivalents of R sulfonyl chloride or R carbonyl chloride and six equivalents of DIEA in NMP. After washing twice with DMF, three times with methanol and drying the resin under vacuum, all compounds were cleaved from the resin by treatment with trifluoroacetic acid (TFA) for 2 h. The resin was then washed several times with acetic acid and DCM. The solution containing the compound was concentrated and dried. The purity of each product was determined using HPLC and structure confirmed using H-NMR and mass spectroscopy (see the Supplementary material section).

Enzymology

LcTS was heterologously expressed and purified [52]; the enzyme was greater than 95% homogenous as determined using sodium dodecylsulfate-polyacrylamide gel electrophoresis (SDS–PAGE). Purified enzyme was stored at −80°C in 1 mM phosphate buffer, pH 7.0, 0.1 mM EDTA. Stock solutions of the inhibitors were prepared in DMSO and stored at −20°C. The inhibitory activity of the compounds versus TS was determined by enzyme assay. The assays were performed spectrophotometrically by following the absorbance at 340 nm, which increases during the TS catalyzed reaction due to the oxidation of CH_2–H_4folate to dihydrofolate. These assays were performed in a Hewlett Packard 8453 UV spectrophotometer equipped with a multicell transporter and thermostated with a circulating bath. Assays were performed at 20°C in the standard assay buffer, which contained 50 mM TES at pH 7.4, 25 mM $MgCl_2$, 6.5 mM formaldehyde, 1 mM EDTA and 75 mM 2-mercaptoethanol. For IC50 calculations, assays were performed with 80 μM dUMP, 0.03 μM TS and 30 μM CH_2–H_4folate. For the K_i calculations the CH_2–H_4folate was varied from 20 μM to 120 μM. The inhibition pattern against dUMP was measured by varying dUMP between 56 μM and 178 μM with CH_2–H_4folate held constant at 32 μM. Reactions were initiated by the addition of enzyme. The K_i values were calculated by plotting the slopes from Lineweaver–Burk analyses versus inhibitor concentration (e.g., Figure 4) [53]. The IC_{50} values were determined by plotting the inverse of the initial velocity against concentration of inhibitor [53]. HTS was purified using affinity column chromatography [54]. The enzyme was greater than 95% homogeneous by SDS–PAGE. HTS was used immediately after purification.

DHFR (EC 1.5.1.3) from bovine liver (Sigma Chemical, St. Louis MO) assays were monitored spectrophotometrically by measuring the decrease in absorbance at 340 nm upon NADPH reduction. Assays were conducted in 50 mM TES, 1 mM EDTA and 75 mM 2-mercaptoethanol,

pH 7 at 25°C. NADPH was used at a concentration of 100 μM, the dihydrofolate concentration was 58 μM, and 0.011 units of enzyme were used per assay (1 unit is the amount required to reduce 1 nmol of dihydrofolate per minute). Assays were initiated with enzyme. Dimethyl sulfoxide (DMSO) was used to deliver inhibitor; the DMSO never exceeded 10% of the reaction volume.

Bovine pancreatic α-chymotrypsin (Sigma) assays were performed by monitoring the hydrolysis of *N*-benzoyl-l-tyrosine ethyl ester (Sigma) [55]. All assays were initiated with enzyme. DMSO was used to deliver the inhibitor and never exceeded 5% of the total reaction volume.

Supplementary material

Additional details on liquid phase syntheses, NMR and MS analyses are published with the online version of this paper.

Acknowledgements

We thank Emilia Caselli for assistance with chymotrypsin assays, Paola Vianello for assistance with logP calculations, and Richard Silverman, D. Lorber, B. Beadle and S. Weston for critical reading of the manuscript. B.K.S. thanks MDL for the ISIS program and the ACD database. Partial support was provided by the Animal Alternatives Program of Procter & Gamble and by Genetics Institute (to B.K.S.), the Howard Hughes Medical Institute through a faculty development grant to Northwestern University (PI J. Larry Jameson), and GM30861 (to D.M.W.). D.T. was partly supported by a doctoral fellowship from the Dipartimento di Scienze Farmaceutiche, Università di Modena. D.T., U.S., D.M.W. and B.K.S. are members of the Drug Discovery Program of Northwestern University.

References

1. Appelt, K., *et al.*, & White, J. (1991). Design of enzyme inhibitors using iterative protein crystallographic analysis. *J. Med. Chem.* **34**, 1925-1934.
2. Wilson, K.P., *et al.*, & Su, M.S. (1997). The structural basis for the specificity of pyridinylimidazole inhibitors of p38 MAP kinase. *Chem. Biol.* **4**, 423-431.
3. Montgomery, J.A., *et al.*, & Ealick, S.E. (1993). Structure-based design of inhibitors of purine nucleoside phosphorylase. 1. 9-(arylmethyl) derivatives of 9-deazaguanine. *J. Med. Chem.* **36**, 55-69.
4. von Itzstein, M., *et al.*, & Penn, C.R. (1993). Rational design of potent sialidase-based inhibitors of influenza virus replication. *Nature* **363**, 418-423.
5. Kick, E.K., *et al.*, & Ellman, J.A. (1997). Structure-based design and combinatorial chemistry yield low nanomolar inhibitors of cathepsin D. *Chem. Biol.* **4**, 297-307.
6. Brady, S.F., *et al.*, & Vacca, J.P. (1998). Discovery and development of the novel potent orally active thrombin inhibitor N-(9-hydroxy-9-fluorenecarboxy) prolyl trans-4-aminocyclohexylmethyl amide (L-372,460): coapplication of structure-based design and rapid multiple analogue synthesis on solid support. *J. Med. Chem.* **41**, 401-406.
7. Zuckermann, R.N. *et al.*, & Moos, W.H. (1994). Discovery of nanomolar ligands for 7-transmembrane G-protein-coupled receptors from a diverse N-(substituted) glycine peptoid library. *J. Med. Chem.* **37**, 2678-2685.
8. Ballinger, M.D., *et al.*, & Wells, J.A. (1998). Selection of heregulin variants having higher affinity for the ErbB3 receptor by monovalent phage display. *J. Biol. Chem.* **273**, 11675-11684.
9. Bartlett, P.A., Shea, G.T., Telfer, S.T. & Waterman, S. (1989). CAVEAT: A program to facilitate the structure derived design of biologically active molecules. In *Molecular Recognition.* (S.M. Roberts, ed). pp182-196. Royal Society of Chemistry, London.
10. Kuntz, I.D., Meng, E.C. & Shoichet, B.K. (1994). Structure-based molecular design. *Accounts Chem. Res.* **27**, 117-123.
11. Toney, J.H., *et al.*, & Hammond, G.G. (1998). Antibiotic sensitization using biphenyl tetrazoles as potent inhibitors of *Bacteroides fragilis* metallo-beta-lactamase. *Chem. Biol.* **5**, 185-196.
12. Burkhard, P., Taylor, P. & Walkinshaw, M.D. (1998). An example of a protein ligand found by database mining: description of the docking method and its verification by a 2.3 Å X-ray structure of a thrombin-ligand complex. *J. Mol. Biol.* **277**, 449-466.
13. Reich, S.H., *et al.*, & White, J. (1992). Design and synthesis of novel 6,7-imidazotetrahydroquinoline inhibitors of thymidylate synthase using iterative protein crystal structure analysis. *J. Med. Chem* **35**, 847-858.
14. Verlinde, C.L. & Hol, W.G. (1994). Structure-based drug design: progress, results and challenges. *Structure* **2**, 577-587.
15. Jones, T.R., *et al.*, & Morse, C.A. (1996). Structure-based design of lipophilic quinazoline inhibitors of thymidylate synthase. *J. Med. Chem.* **39**, 904-917.
16. Bohacek, R.S., McMartin, C. & Guida, W.C. (1996). The art and practice of structure-based drug design: a molecular modeling perspective. *Med. Res. Rev.* **16**, 3-50.
17. Ren, J., *et al.*, & Stammers, D. (1995). High resolution structures of HIV-1 RT from four RT-inhibitor complexes. *Struct. Biol.* **2**, 293-302.
18. Shoichet, B.K., Perry, K.M., Santi, D.V., Stroud, R.M. & Kuntz, I.D. (1993). Structure-based discovery of inhibitors of thymidylate synthase. *Science* **259**, 1445-1450.
19. Arevalo, J.H., Taussig, M.J. & Wilson, I.A. (1993). Molecular basis of crossreactivity and the limits of antibody–antigen complementarity. *Nature* **365**, 859-863.
20. Badger, J., Minor, I., Oliveira, M.A., Smith, T.J. & Rossmann, M.G. (1989). Structural analysis of antiviral agents that interact with the capsid of human rhinovirus. *Proteins* **6**, 1-19.
21. Mehanna, A.A. & Abraham, D.J. (1990). Comparison of crystal and solution hemoglobin binding of selected antigelling agents and allosteric modifiers. *Biochemistry* **29**, 3944-3952.
22. Bolin, J.T., Filman, D.J., Matthews, D.A., Hamlin, R.C. & Kraut, J. (1982). Crystal structures of *E. coli* and *L. casei* DHFR refined to 1.7 Angstrom resolution. 1. General features and binding of methotrexate. *J. Biol. Chem.* **257**, 13650-13662.
23. Rutenber, E., *et al.*, Stroud, R.M. (1993). Structure of a non-peptide inhibitor complexed with HIV-1 protease. *J. Biol. Chem.* **268**, 15343-15346.
24. Malby, R.L., *et al.*, & Colman, P.M. (1994). The structure of a complex between the NC10 antibody and influenza virus neuraminidase and comparison with the overlapping binding site of the NC41 antibody. *Structure* **2**, 733-746.
25. Mattos, C., Rasmussen, B., Ding, X., Petsko, G.A. & Ringe, D. (1994). Analogous inhibitors of elastase do not always bind analogously. *Nat. Struct. Biol.* **1**, 55-58.
26. Radzicka, A. & Wolfenden, R. (1995). A proficient enzyme. *Science* **267**, 90-93.
27. Hardy, L.W. & Nalivaika, E. (1992). Asn177 in *Escherichia coli* thymidylate synthase is a major determinant of pyrimidine specificity. *Proc. Natl Acad. Sci. USA* **89**, 9725-9729.
28. DesJarlais, R.L., *et al.*, & Craik, C.S. (1990). Structure-based design of nonpeptide inhibitors specific for the human immunodeficiency virus 1 protease. *Proc. Natl Acad. Sci. USA* **87**, 6644-6648.
29. Bodian, D.L., Yamasaki, R.B., Buswell, R.L., Stearns, J.F., White, J.M. & Kuntz, I.D. (1993). Inhibition of the fusion-inducing conformational change of the influenza hemagglutinin by bensoquinones and hydroquinones. *Biochemistry* **32**, 2967-2978.
30. Finer-Moore, J., Fauman, E.B., Foster, P.G., Perry, K.M., Santi, D.V. & Stroud, R.M. (1993). Refined structures of substrate-bound and phosphate-bound thymidylate synthase from *Lactobacillus casei*. *J. Mol. Biol.* **232**, 1101-1116.
31. Meng, E.C., Shoichet, B. & Kuntz, I.D. (1992). Automated docking with grid-based energy evaluation. *J. Comp. Chem.* **13**, 505-524.
32. Shoichet, B.K., Leach, A.R. & Kuntz, I.D. (1999). Ligand solvation in molecular docking. *Proteins* **34**, 4-16.
33. Lorber, D.M. & Shoichet, B.K. (1998). Flexible ligand docking using conformational ensembles. *Prot. Science* **7**, 151-158.
34. Leo, A.J. (1993). Calculating LogP(Oct) from structures. *Chem. Rev.* **93**, 1281-1306.
35. Lu, W., *et al.*, & Laskowski, M., Jr. (1997). Binding of amino acid sidechains to S1 cavities of serine proteinases. *J. Mol. Biol.* **266**, 441-461.
36. Ariens, E.J. (1971). Drug Design in *Drug Design* vol. 1, pp. 177 (E.J. Ariens, ed). Academic Press, New York.
37. Gangjee, A., Mavandadi, F., Kisliuk, R.L., McGuire, J.J. & Queener, S.F. (1996). 2-Amino-4-oxo-5-substituted-pyrrolo[2,3-d]pyrimidines as nonclassical antifolate inhibitors of thymidylate synthase. *J. Med. Chem.* **39**, 4563-4568.
38. Costi, M.P. (1998). Thymidylate synthase inhibition: a structure-based rationale for drug design. *Med. Res. Rev.* **18**, 21-42.
39. Shoichet, B.K. & Kuntz, I.D. (1996). Predicting the structures of protein complexes: a step in the right direction. *Chem. Biol.* **3**, 151-156.
40. Strynadka, N.C., *et al.*, & James, M.N.G. (1996). Molecular docking programs successfully predict the binding of a beta-lactamase inhibitory protein to TEM-1 beta-lactamase. *Nat. Struct. Biol.* **3**, 233-239.

41. Stout, T.J., *et al.*, & Costi, M.P. (1999). Structure-based design of inhibitors specific for bacterial thymidylate synthase. *Biochemistry* **38**, 1607-1617.
42. Montfort, W.R., *et al.*, & Stroud, R.M. (1990). Structure, multiple site binding, and segmental accommodation in thymidylate synthase on binding dUMP and an anti-folate. *Biochemistry* **29**, 6964-6976.
43. Liu, L. & Santi, D.V. (1993). Exclusion of 2′-deoxycytidine 5′-monophosphate by asparagine 229 of thymidylate synthase. *Biochemistry,* **32**, 9263-9267.
44. Weber, P.C., Pantoliano, M.W. & Thompson, L.D. (1992). Crystal structure and ligand-binding studies of a screened peptide complexed with streptavidin. *Biochemistry* **31**, 9350-9354.
45. Scheidig, A.J., Hynes, T.R., Pelletier, L.A., Wells, J.A. & Kossiakoff, A.A. (1997). Crystal structures of bovine chymotrypsin and trypsin complexed to the inhibitor domain of Alzheimer's amyloid beta-protein precursor (APPI) and basic pancreatic trypsin inhibitor (BPTI): engineering of inhibitors with altered specificities. *Protein Sci.* **6**, 1806-24.
46. Shoichet, B., Bodian, D.L. & Kuntz, I.D. (1992). Molecular docking using sphere descriptors. *J. Comp. Chem.* **13**, 380-397.
47. Meng, E.C., Gschwend, D.C., Blaney, J.M. & Kuntz, I.D. (1993). Orientational sampling and rigid-body minimization in molecular docking. *Proteins* **17**, 266-278.
48. Gilson, M.K. & Honig, B.H. (1987). Calculation of electrostatic potentials in an enzyme active site. *Nature* **330**, 84-86.
49. Ferrin, T.E., Huang, C.C., Jarvis, L.E. & Langridge, R. (1988). The MIDAS display system. *J. Mol. Graph.* **6**, 13-27.
50. Rink, H. (1987). Solid-phase synthesis of protected peptide-fragments using a trialkoxy-diphenyl-methylester resin. *Tetrahedron Lett.* **28**, 3787-3790.
51. Blankenmeyer-Menge, B., Nimtz, M. & Frank, R. (1990). An efficient method for anchoring Fmoc-amino acids to hydroxyl-functionalized solid supports. *Tetrahedron Lett.* **31**, 1701-1704.
52. Climie, S. & Santi, D.V. (1990). Chemical synthesis of the thymidylate synthase gene. *Proc. Natl Acad. Sci. USA* **87**, 633-637.
53. Segel, I.H. (1975) *Enzyme Kinetics* Wiley, New York.
54. Davisson, V.J., Sirawaraporn, W. & Santi, D.V. (1989). Expression of human thymidylate synthase in *Escherichia coli*. *J. Biol. Chem.* **264**, 9145-9148.
55. Weston, G.S., Blazquez, J., Baquero, F. & Shoichet, B.K. (1998). Structure-based enhancement of boronic acid inhibitors of AmpC beta-lactamase. *J. Med. Chem.* **41**, 4577-4586.

Because *Chemistry & Biology* operates a 'Continuous Publication System' for Research Papers, this paper has been published via the internet before being printed. The paper can be accessed from http://biomednet.com/cbiology/cmb – for further information, see the explanation on the contents pages.